

SEASONAL CAVE AIR VENTILATION CONTROLLING VARIATION IN CAVE AIR P_{CO_2} AND DRIP WATER GEOCHEMISTRY AT INAZUMI CAVE, OITA, NORTHEASTERN KYUSHU, JAPAN

Tatsuro Shindoh^{1, c}, Taketoshi Mishima², Yumiko Watanabe¹, Shinji Ohsawa², and Takahiro Tagami¹

Abstract

To compare the influence of cave air P_{CO_2} and drip rate on the drip water geochemistry, approximately one year of cave air monitoring and sampling of drip water were conducted at Inazumi Cave, Oita, northeastern Kyushu, Japan, from February to December 2014. The monitoring revealed that temperature dependent cave air ventilation controlled distinct seasonal variation in the cave air P_{CO_2} and minor variation in temperature and relative humidity with increasing distance from the cave entrance. In addition to traditional sampling of drip water, novel sampling methods were designed to compare the influence of the P_{CO_2} and the drip rate on the karstic and drip water geochemistry. The chemical analysis indicated that the karstic and drip water instantaneously outgassed CO_2 once in contact with low cave air P_{CO_2} . The drip rate alone, however, had less significant influence on the drip water geochemistry than the P_{CO_2} . The drip water P_{CO_2} was repeatedly lower than cave air P_{CO_2} , and this is probably due to prior calcite precipitation, to a temporal increase of the cave air P_{CO_2} by anthropogenic CO_2 , or to storage conditions of the sample; all of which cause alteration of drip water geochemistry from the original state.

Introduction

Stalagmite, a limestone cave deposit, has been recognized as a useful terrestrial paleoclimate archive because the variety of proxies preserved in lamina provides valuable sources for interpretation of climate change. For instance, variations in $\delta^{18}O$ have been interpreted as reflecting variations in meteoric water sources (e.g., Wang et al., 2001), the intensity of Asian monsoon, and amount of rainfall through the time (e.g., Burns et al., 2002; Watanabe et al., 2010; Cai et al., 2010). Moreover, variations in trace elements such as Mg and Sr (e.g., Treble et al., 2003; Johnson et al., 2006) and lamina thickness (e.g., Proctor et al., 2000, 2002) and its texture and fabrics (e.g., Matthey et al., 2008; Boch et al., 2011) have been used for reconstruction of terrestrial paleoclimate.

Although these proxies are regarded as related to meteorological and climatological information outside limestone caves, they might be altered by a kinetic effect, "in-cave processes" including evaporation, CO_2 degassing, and $CaCO_3$ precipitation from drip water (e.g., Hendy, 1971; Mickler et al., 2006), which are controlled by variations in cave air temperature, relative humidity, and P_{CO_2} . Isotopes and geochemistry of the deposited $CaCO_3$ in stalagmites are, therefore, strongly affected by a complex interplay that the drip water has experienced in the cave environment. To understand the complex interplay, cave air monitoring can help to narrow down the variables that affect the isotopic and geochemical signatures of the deposited $CaCO_3$ and the drip water.

Spötl et al. (2005) conducted pioneering work in the Obir Cave, Austria, and reported seasonal variation in the cave air P_{CO_2} as the main variable affecting CO_2 degassing and $CaCO_3$ precipitation from the drip water. Subsequent studies have revealed similar trends (e.g., Banner et al., 2007; Matthey et al., 2010; Boch et al., 2011; Wang et al., 2016), and the variation in P_{CO_2} has increasingly gained attention as an important variable controlling drip water kinetics.

However, some laboratory experiments have demonstrated that drip rate is an important variable affecting the kinetics of the drip water geochemistry. Day and Henderson (2011) conducted a $CaCO_3$ precipitation experiment in a cave analog condition with three different drip rates, slow, moderate, and fast, and reported that the moderate drip rate produced the greatest amount of $CaCO_3$ deposition, suggesting that the drip rate strongly affects the lamina thickness of stalagmites.

Both the cave air P_{CO_2} and the drip rate are important variables controlling the drip water geochemistry and speleothem growth dynamics. Interpreting the influence of the cave air P_{CO_2} and the drip rate on the geochemistry provides better understanding of how the geochemistry is altered in a natural cave environment.

In this study, we compare the influence of the cave air P_{CO_2} and the drip rate on the drip water geochemistry by applying novel sampling techniques to collect drip water in the course of the monitoring period at the Inazumi Cave, Japan. This study and the novel sampling techniques suggest that variation in the cave air P_{CO_2} controls drip water geochemistry more than the drip rate in the Inazumi Cave.

¹Division of Earth and Planetary Sciences, Graduate School of Sciences, Kyoto University, Kyoto, 606-8502, Japan

²Beppu Geothermal Research Laboratory, Institute of Geothermal Sciences, Graduate School of Science, Kyoto University, Oita, 874-0903, Japan

^c Corresponding Author: shindoh.tatsuro.47r@st.kyoto-u.ac.jp

Site Description

The Inazumi Cave is located at Bungo'ono, Oita prefecture, northeastern Kyushu, Japan (32°54'00.4"N, 131°32'31.8"E). The tourist cave consists of two approximately 300 m long meandering branches from their intersection, Suichu Cave and Shinsei Cave (Fig. 1A). The branches were previously separated, but are currently connected by artificial passages for tourism. The Suichu Cave contains a cave river flowing out of point D to the opening A, and some chambers and passages are partially underwater. There are two openings to Inazumi Cave (A and B in Fig. 1B). Opening B is the entrance point for tourists, while opening A is a river channel with no sidewalk for visitors. This study used the opening B for entering to all passages and chambers of the cave.

The Inazumi Cave is characterized by a history of being completely flooded. Blockage of all cave openings by pyroclastic flow deposited by the Aso-4 eruption occurred ca. 90,000 years ago, resulting in loss of all drain outlets and filling up of the entire cave by river water (Fuji and Nishida, 1999). The pyroclastic flow deposits are now all removed by erosion by the Nakatsuburei River near the Inazumi Cave, and the water level in the cave is low, enabling visits by tourists on the sidewalk. Occasional complete cave flooding has been reported during heavy rain periods. Some erosional features and mud coatings over the whole cave and on numerous speleothems are evidence of previous cave flooding.

Figure 1C presents a hythergraph of Ume, a meteorological station about 15 km away from the Inazumi Cave, indicating mean annual temperature of 14.3°C and mean annual precipitation of 185.8 mm yr⁻¹, ranging from 44.1 in December to 359.2 mm in August for 1981–2010. The climate of this region is characterized by distinct seasonality due to the East Asian monsoon, with higher precipitation and temperatures in summer and autumn and lower in winter and spring. Flooding in Inazumi Cave has been reported mainly during summer and autumn, when many tourists visit Inazumi Cave.

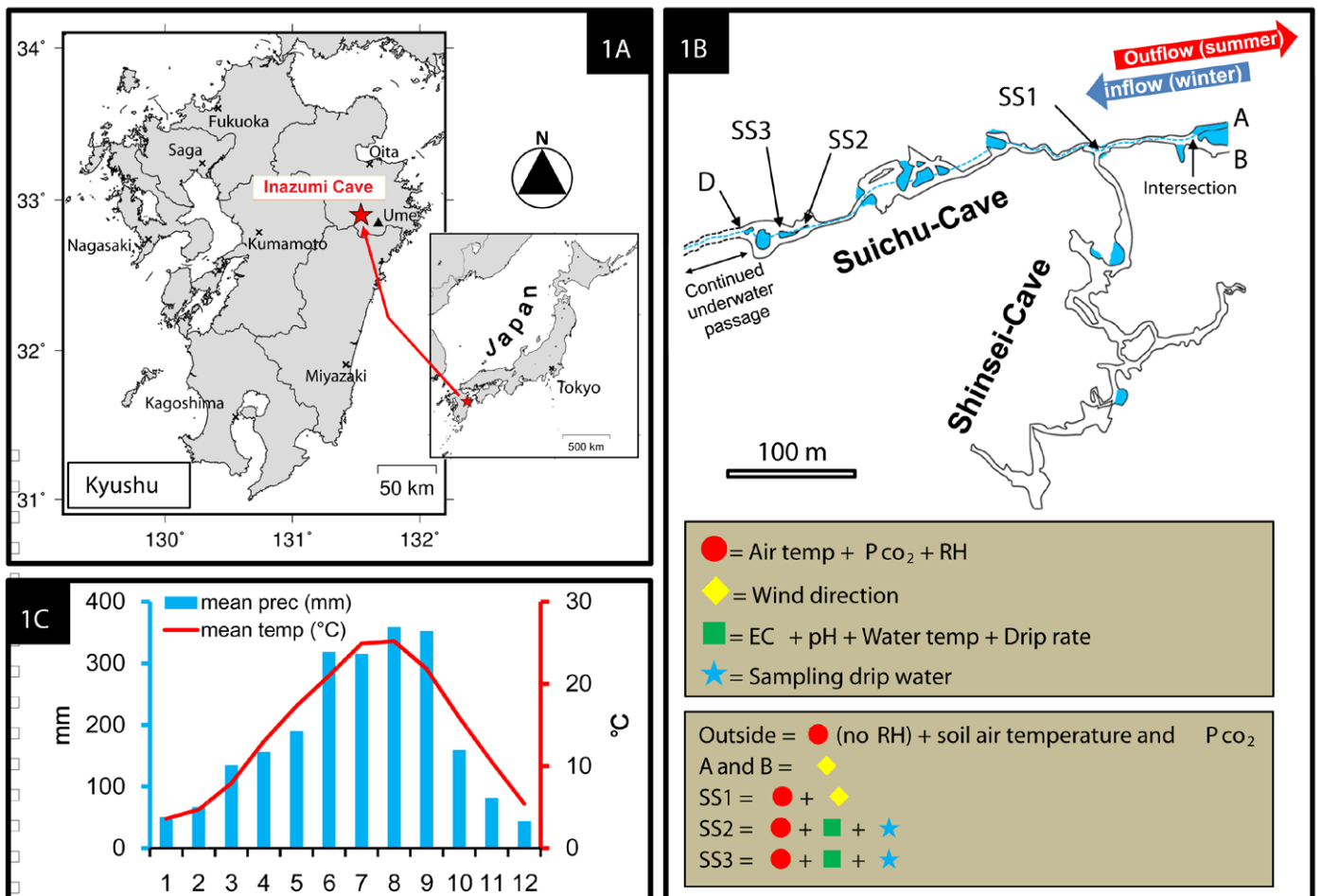


Figure 1. (1A): Location of Inazumi Cave indicated by red star. (1B): Plan view of Inazumi Cave with the locations of monitoring and sampling sites. See symbols below the cave map for details of the monitoring at each site. Light blue-colored parts in the cave map are underwater passages and chambers, and the dashed light blue line is the cave-river channel flowing out of point D in Suichu Cave to the opening A. Blue and red arrows above the opening A and B indicate how the direction of the cave air differed by seasons. (1C): A hythergraph at Ume, the closest meteorological station to Inazumi Cave.

Materials and Methods

Cave air monitoring and drip water sampling were conducted for three days and two nights in Inazumi Cave nearly every month from February to December 2014. No monitoring was conducted in September, but monitoring and sampling of the drip water were conducted at the beginning and end of October instead (OI and OII, respectively, in figures). Cave air monitoring was initiated at 11:00 on the first day and ended at 15:00 on the third day, making 52 hours in total for every monitoring period. As we define daytime and night time as the time periods from 7:00 to 17:00 and from 18:00 to 6:00 respectively, the first day of the monitoring period is shorter than other periods.

Cave Air Monitoring

Cave air temperature, relative humidity and P_{CO_2} were logged at three monitoring sites labeled SS1, SS2, and SS3 (Fig. 1B). The air temperature and P_{CO_2} but not RH outside the cave were also logged. The air temperature and RH were logged using humidity logger LR5001 (accuracy $\pm 0.5^\circ\text{C}$ from 0.0 to 35.0°C for temperature and $\pm 5\%$ at 20–30°C / 10–50% for RH). The air P_{CO_2} was logged using a SenseAir portable CO_2 logger (± 20 ppm at 20 °C and 1013 hPa).

Soil air temperatures and P_{CO_2} below the surface of the soil were measured daytime and night time of every monitoring period. An electrode with a silicon tube was installed at 1 m depth below the soil surface about 50 m away from the cave entrance. The electrical resistance value was measured and converted into the soil air temperature. The soil air P_{CO_2} was measured from a silicon tube attached to the electrode using a CO_2 detector (Gastec Corp.).

The cave air direction was visually recorded using smoke from incense sticks at 5, 100, and 200 cm from the floor of the passage, labeled respectively as lower, middle, and upper sections, at SS1 and the openings A and B. The flow for the opening A was recorded at the intersection of the two openings because there was no accessible passage for the opening A (Fig. 1B). Using smoke from incense sticks is a method described by Ohsawa (2009) and Hasegawa et al. (2014).

In-Situ Measurement of Drip Water

The water temperature, pH, electrical conductivity, and drip rate were measured at two dripping sites SS2 and SS3. Water temperature and pH were measured using a pH meter (± 0.01 for pH; ± 0.1 °C for water temperature, D-50 series; Horiba Ltd.). The EC was measured using a compact conductivity meter ($\pm 2\%$ full scale for each range, B-711; Horiba Ltd.). The drip rate was measured using a stopwatch and a 4.9 ml PET tube.

Sampling of Water

Drip water sampling by a novel sampling approach was conducted at sites SS2 and SS3 each day and night time during the monitoring periods. At SS2, a series of three handrails is installed where drip water hits the handrails in order, and the drip water before and after hitting each of the handrails was collected and labeled respectively as SS2U, SS2M1, SS2M2, SS2M3, and SS2L from the top to the bottom. (Handrails are labeled respectively as Handrails 1, 2, and 3 from the top to the bottom; see Fig. 2A-1 for a schematic diagram and the image in Fig. 2A-2). Sampling of SS2M3 only started from May. The drip water is supplied from a vein-shaped and cream-colored stalactite and flows along the stalactite's flank (Fig. 2A-3). Small dome-like and brown stalagmites are formed on each of the handrails at the drip-water contact and gradually become smaller in the sequential order of the handrails (Fig. 2A-1 and 2A-4). Vertical distances between the vein-shaped stalactite and the handrails are as follows: 105 cm between the vein-shaped stalactite and the Handrail 1; 34 cm between the Handrails 1, 2, and 3, and 7 cm between the Handrail 3 and the cave floor.

At SS3, a sandblasted glass tube was installed on a point where the seepage water drips (Figs. 2B-1 and 2B-2). The seepage water before and after hitting the glass tube was collected and labeled respectively as SS3U, SS3M, and SS3L from the top down. This sampling method is similar to site SS2. In addition, the water before dripping was collected with a novel sampling method illustrated in Figure 2B-4 and 2B-5 and labeled as WBD. This method is designed to obtain a purer chemical signature of the water within the carbonate rock matrix above the cave by blocking the water-cave air interaction. Before instrument usage, pre-existing air inside the sampling bag was completely removed, and the silicon tube part was tightly clamped to prevent the sampling bag from collecting ambient air. The rubber part was attached to the tip of the stalactite and the clamp was open, enabling the WBD sample to flow into the bag. After sampling a sufficient amount of the WBD for chemical analysis (ca. 100 ml), the sampling bag was tightly closed, and the rubber part was removed from the stalactite. Note that the water supplied from the stalactite at SS3 is seeping from the stalactite's core, not flowing along the stalactite's flank. All drip water at SS2 and SS3 was collected in 4.9 ml PET tubes with no head space, capped by a silicon plug, and sealed tightly using vinyl tape. All samples were kept in storage in a refrigerator before chemical analysis.

Chemical Analysis

Cations (Ca, Mg, Na, and K) and anions (Cl, F, SO_4 , and NO_3) of the samples were measured using ion chromatography (ICS-1100; Dionex Corp.) at the Department of Geology and Mineralogy of Kyoto University. Concentration

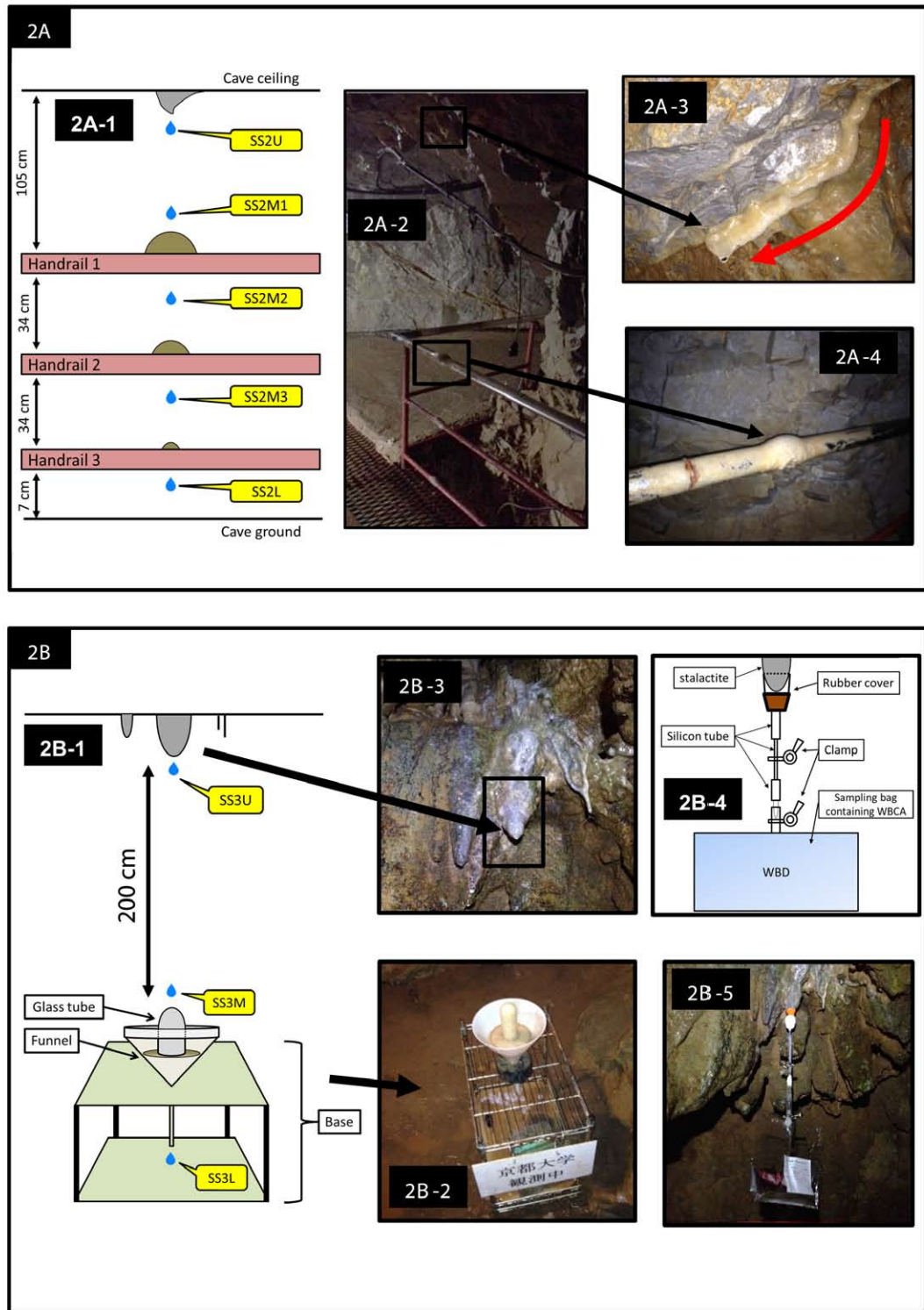


Figure 2. Schematic diagrams and photographs of the novel sampling method of the drip water at SS2 and SS3. (2A-1): A series of three handrails (2A-2) exists at SS2, with the drip water hitting the handrails in the sequential order of the handrails. Samples of water before and after hitting the handrails were collected. The water is supplied from a vein-shaped and cream-colored stalactite (2A-3). The red arrow on the photograph indicates the flow direction of the water fed from the stalactite. Brown dome-shaped stalagmites are formed on each handrail (2A-4), and the size becomes smaller in sequential order of the handrails. Vertical distances between the vein-shaped stalactite and the handrails are the following: 105 cm between the vein-shaped stalactite and the handrail 1, 34 cm between the handrails 1, 2, and 3, and; 7 cm between the handrail 3 and the cave ground. (2B-1): A sandblasted glass tube was placed on the dripping point at SS3, and the water before and after it hit the glass tube was sampled. (2B-2): A photograph of the glass tube at SS3. (2B-3): A photograph of the conical stalactite. The stalactite enclosed by a black square was used for collecting dripping water and the WBD. (2B-4): Schematic diagram of sampling the WBD. (2B-5): A photograph of sampling the WBD.

of HCO_3^- was determined by a spectrometry method described by Mishima et al. (2009). The method is designed for quantitative analysis of HCO_3^- in a small amount (0.1–0.3 mL) of environmental water such as drip water.

Mishima's method uses bromocresol green solution for measuring HCO_3^- in the dip water. The absorption spectra of BCG are varied at different pHs: 445 nm at acidic and 616 nm at basic pH. Combining the Henderson–Hasselbalch equation and Beer and Lambert law produces the following formula

$$\text{pH} = \text{p}K_a + \log \left[\frac{\frac{A_{616}}{e_{22}} - \frac{e_{21}}{A_{445}}}{\frac{A_{445}}{e_{11}} - \frac{e_{12}}{A_{616}}} \right] \quad (1)$$

(1) where $\text{p}K_a$ is the dissociate constant determined by water temperature, A_{445} and A_{616} respectively denote the absorption spectra at acidic and basic pH, ϵ_{11} and ϵ_{12} respectively represent the absorption coefficients at 445 nm, and ϵ_{21} and ϵ_{22} are those at 616 nm. $\epsilon_{22}/\epsilon_{11}$, $\epsilon_{12}/\epsilon_{11}$, and $\epsilon_{21}/\epsilon_{11}$ in Equation (1) will be constant if the water temperature is constant. These variables can be expressed respectively as a, b, and c, and the Equation (1) can be rearranged to

$$[\text{HCO}_3^-] = [\text{H}^+] K_a \frac{a - b \left(\frac{A_{616}}{A_{445}} \right)}{\left(\frac{A_{616}}{A_{445}} \right) - c} \quad (2)$$

(2) In Equation (2), $[\text{HCO}_3^-]$ and $[\text{H}^+]$ respectively represent bicarbonate- and hydrogen-ion concentrations in mg L^{-1} . Equation (2) was used to determine HCO_3^- of the drip water sample.

For obtaining a calibration curve, 0.04 w/v % of bromocresol green solution (Wako Pure Chemical Inds. Ltd.), 0.1 mol L^{-1} HCl and 500 mg/L HCO_3^- standard solutions were prepared from sodium hydrogen carbonate (NaHCO_3 , Special Grade; Wako Pure Chemical Inds. Ltd.). The 0.1 mol L^{-1} HCl was diluted to 1000 times with de-ionized water to prepare 0.1 mmol L^{-1} HCl solution. Subsequently, 0.38 mL BCG and 10 mL of the diluted 0.1 mmol L^{-1} HCl were aliquoted into seven 12 mL PET tubes. The 500 mg/L NaHCO_3 standard solution was diluted with de-ionized water to prepare 50, 100, 150, 200, 250, and 300 mg L^{-1} standard solutions. Of each standard solution, 0.2 mL was added to the solutions containing the BCG and HCl. The mixture containing the BCG, HCl, and HCO_3^- standards were agitated gently and settled for at least 5 minutes until the color stabilized. After 5 minutes, the absorbance ratios A_{616}/A_{445} of the solutions was measured using a spectrophotometer (UV-1800; Shimadzu Corp.). The obtained absorbance ratio was provided using Japan Poladigital's DeltaGraph to obtain the calibration curve. Determining HCO_3^- of drip water samples followed the same procedure: 0.2 mL of the drip water sample was added to the solution of 0.38 mL of BCG and 10 mL of the 1000-times diluted HCl. Then the absorbance of the drip water was measured using the same spectrophotometric method. As equilibrium concentrations obtained using these two methods, Mishima's method obtained $152.2 \pm 1.7 \text{ mg/L}$ (1σ) and the traditional neutralization titration obtained $154.0 \pm 1.1 \text{ mg/L}$ (1σ).

The calcite saturation index ($\text{SI}_{\text{calcite}}$) and the drip water P_{CO_2} were calculated using software (PHREEQC ver. 3; Parkhurst and Appelo, 2013). A CaCO_3 -precipitation test using a sandblasted glass plate was conducted at different dripping sites of Inazumi Cave, and the CaCO_3 precipitated on the glass plate was identified as calcite using Raman spectroscopy at the Department of Geology and Mineralogy of Kyoto University (unpublished data). Therefore, the $\text{SI}_{\text{calcite}}$, not the $\text{SI}_{\text{aragonite}}$, was used. No data of water temperature and pH of the WBD samples were obtained because of the unique sampling method. Instead, the temperature and pH of SS3U were used for calculation of $\text{SI}_{\text{calcite}}$ and drip water P_{CO_2} of the WBD as reference values.

Results

Air Monitoring

Figure 3A presents time series variation in the cave air temperature, RH, and P_{CO_2} at the three monitored sites. The outside air temperature was variable, ranging from -0.5 in March to 31.9°C in July, the lowest and largest values respectively. The air temperature and RH inside the cave gradually stabilized with increasing distance from the cave entrance. The air temperature and RH at SS1 indicated a seasonal variation, ranging from 12.9 to 16.8°C for temperature and from 77.6% to 100% for RH. At SS2 and SS3, the deepest localities of the Suichu Cave, the temperature and RH were stable, maintaining $16 \pm 0.2^\circ\text{C}$ and 100% through all monitoring periods. The cave air P_{CO_2} indicated distinct seasonal variation with increasing distance from the cave entrance, ranging from 371 to 3216 ppm at SS1, from 856 to 7073 ppm at SS2 and from 892 to 6788 ppm at SS3, respectively. The extreme increase of the P_{CO_2} at SS2 and SS3 at the end of monitoring period on February 2014 is due to a long stay of numerous visitors. The outside air P_{CO_2} , on the

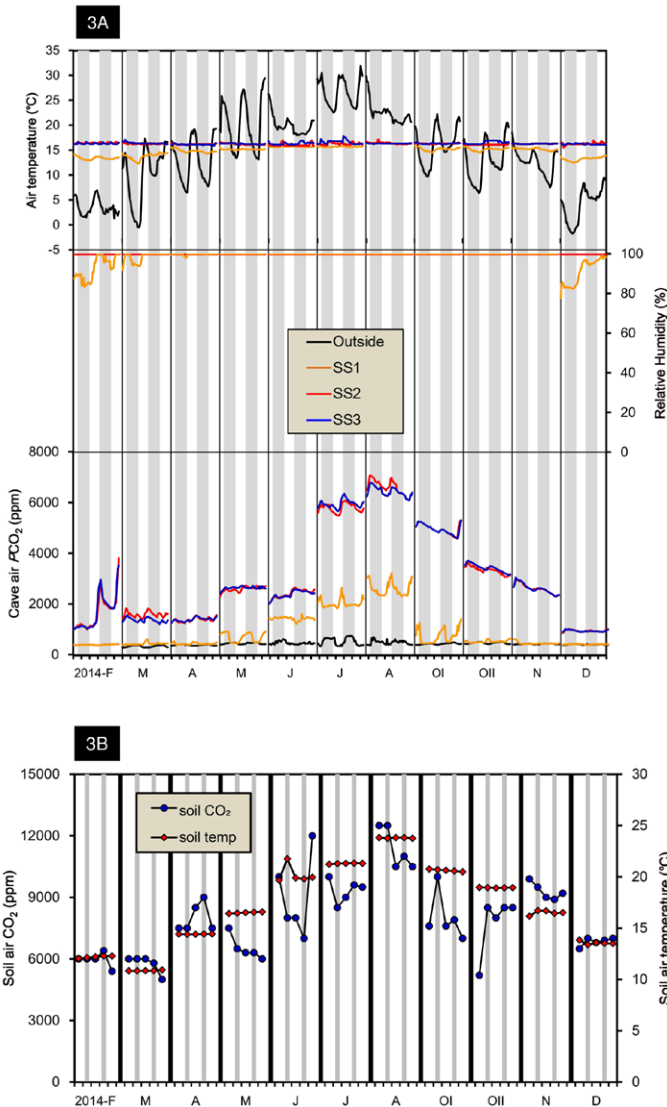


Figure 3. (3A): Time series variation in logged cave air temperature, relative humidity, and P_{CO_2} at sites monitored for 52 hours monthly from February to December 2014. Gray bars indicate night time from 18:00 to 6:00 and white ones indicate daytime from 7:00 to 17:00. Note that RH at SS2 and SS3 always show 100% during the course of this study and that first white bars at each monitoring periods are narrower than others since the onset time of each monitoring was began at 11:00. (3B): Time series variation in measured soil air temperature and P_{CO_2} . The gray and white bars are the same as in 3A.

other hand, showed 429 ± 77 ppm through all monitoring periods, more stable than the cave air.

Soil air temperature and P_{CO_2} showed seasonal variation, with high values during the warm season and low values during the cold season (Fig. 3B). The air P_{CO_2} showed irregular diurnal fluctuation, whereas the temperature showed little diurnal variation.

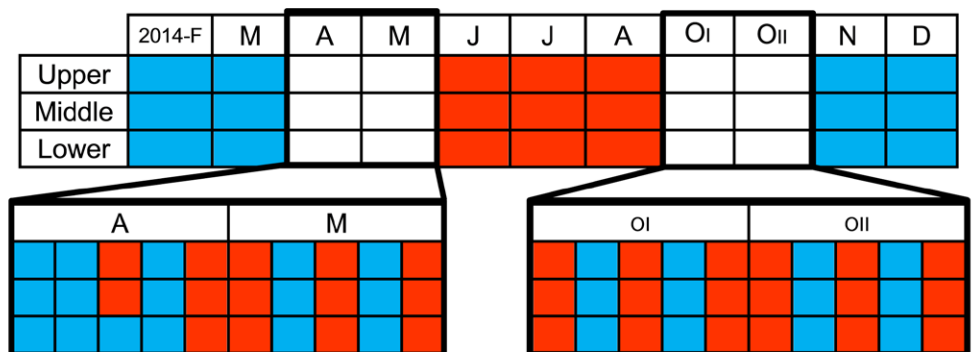
Figure 4A summarizes time series variation in the cave air direction at SS1 and indicates seasonal variation as the overall trend and diurnal variation in April, May, October I and II. While outside air flowed into the cave during the cold season, the air flowed out of the cave during warm period. Smoke gradually diffused from the tip of the incense stick, but showed the same direction at all three recorded sections in the course of this study. No differences in the air flow were found depending on altitude in the cave passage, except for April, when the air flow at lower section moved in the opposite direction than the air in middle and upper sections (Fig. 4). The cave air of all three recorded sections at the opening B, on the other hand, always flowed out of the cave regardless of season, and the smoke diffused in all directions to far from the opening, making it difficult to identify the flow direction. This might be caused by the opening B having a large chamber where cave air was easily scattered in all directions. The cave air flow at the intersection of the opening A and B showed the same pattern observed at SS1. During cold season, in particular, we observed that air was constantly supplied from the opening A, with a narrow passage, suggesting that the cave air ventilation regime in Inazumi Cave is exclusively controlled by opening A's air circulation.

In Situ Measurement of Drip Water

Figures 5A and 5B show time series variations in in situ measurement of drip water at SS2 and SS3, respectively. Water temperature at both of SS2 and SS3 was stable and maintained $16 \pm 0.2^\circ C$ during the course of this research. EC at SS2 and SS3 showed seasonal variation, with high values in the warm season and low values in the cold season. Particularly, in the cold season, EC decreased in the sequential order of the handrails and glass

■ = inflow ■ = outflow

Figure 4. Variation in the cave air direction at upper, middle, and lower sections of the cave passage at SS1 during the monitoring periods. Blue boxes indicate inflow, incursion of fresh air into the cave, and red ones are outflow, release of the cave air to outside. April, May, October I and II showed distinct diurnal variation. The direction of cave air in other months showed the uniform direction at all recorded sections in daytime and night time.



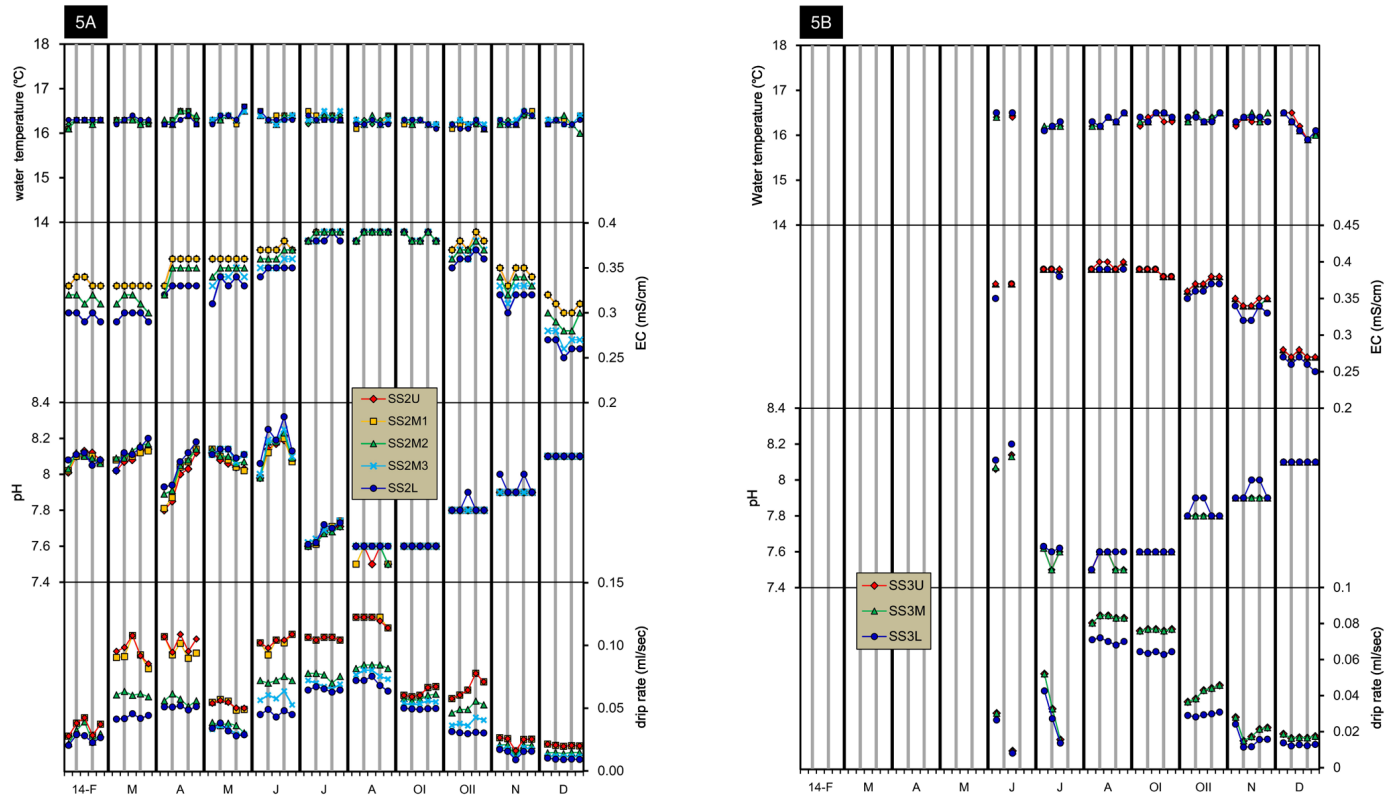


Figure 5. Time series variation in water temperature, EC, pH, and drip rate of the drip water at SS2 (5A) and SS3 (5B). At SS3, there was no supply of drip water from February to May 2014, and the measurement was initiated from June. No data for the WBD were obtained due to the novel sampling method. The white and gray bars are same as Figure 3

tube. The pH was lower in the warm season and higher in the cold season with minor sequential differences. Minor diurnal variation in EC and pH were measured during the course of this study. The drip rate at SS2 from February to July illustrate a slow-and-fast cycle and gradually decreased from August to December. At SS3, the supply of drip water ceased from February to May, was temporarily restored during June and July, and was completely restored in August, with a decreasing trend toward December. The drip rate decreased in the sequential order of the handrails and glass tube; in other words, SS2U and SS3U were the fastest; SS2L and SS3L were the slowest.

Chemical Analysis

Figures 6A and 6B provide time series variations in the chemical analysis of the drip water at SS2 and SS3 respectively. As an overall trend, HCO_3^- and Ca^{2+} at SS2 and SS3 indicated seasonality, with high concentration in the warm season and low concentration in the cold season. The highest HCO_3^- and Ca^{2+} were measured in August, and their concentration were 265.9 mg/L and 89.3 mg/L, respectively at SS2U and 262.4 mg/L and 89.3 mg/L, respectively at the WBD. The lowest were measured in December with concentrations of 55.5 mg/L and 8.0 mg/L at SS2L and 86.0 mg/L and 23.6 mg/L at SS3L. HCO_3^- and Ca^{2+} decreased in the sequential order of the handrails and glass tube during the cold season, with the largest variation in December but minor effects during the warm season. HCO_3^- of the WBD indicated a pronounced difference from SS3U in November and December. The SS2 result in March showed a different pattern from that of other periods, probably because the PET tube was poorly capped with some head space causing undesirable CO_2 degassing while in storage. Other chemical elements including Mg, Na, K, F, Cl, NO_3^- , and SO_4^{2-} were measured and showed no seasonal variation through all monitoring periods.

$\text{SI}_{\text{calcite}}$ at SS2 and SS3 showed seasonal variation, with high values in the cold season and low in the warm season, but had a positive value ($\text{SI}_{\text{calcite}} > 0$) all the time except for some of SS2M2, 3, and L in December. The drip water P_{CO_2} at SS2 and SS3 also indicated distinct seasonality, with high values during the warm season and low values during the cold season. It was frequently lower than the cave air P_{CO_2} , with the largest difference in August. Minor diurnal variations in $\text{SI}_{\text{calcite}}$ and the drip water P_{CO_2} were measured.

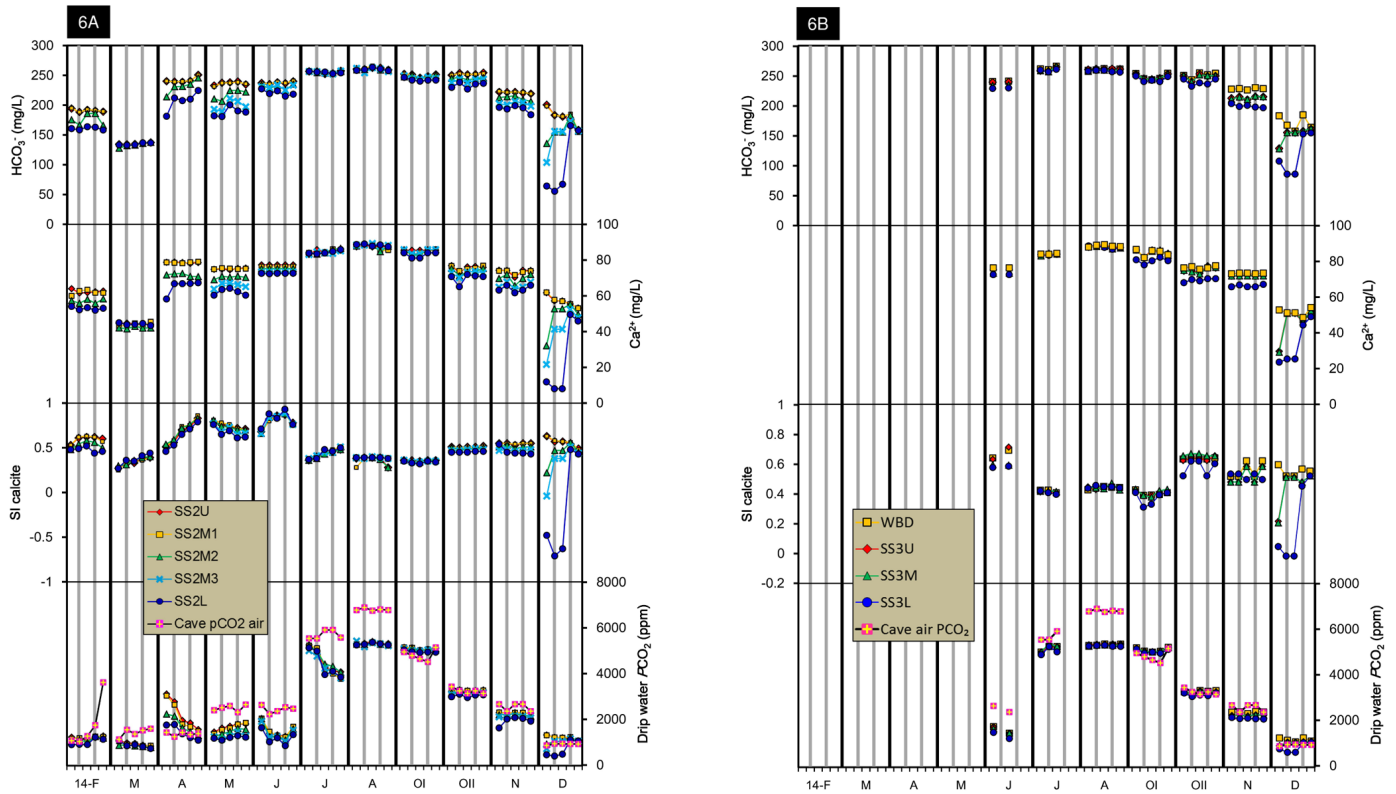


Figure 6. Time series variation in HCO_3^- , Ca^{2+} , $\text{SI}_{\text{calcite}}$ and drip water P_{CO_2} at SS2 (6A) and SS3 (6B). Note that water temperature and pH of SS3U were used for calculation of P_{CO_2} and $\text{SI}_{\text{calcite}}$ of the WBD as the reference values. The white and gray bars are same as Figure 3.

Discussion

Cave Air Ventilation

Our cave air monitoring revealed not only distinct seasonal, but also diurnal, air ventilation exclusively controlled by opening A. The diurnal ventilation observed in April, May, and October I and II suggests that the temperature difference between external and internal atmosphere of the cave drives air circulation, hence ventilation, as reported by numerous studies (e.g., Spötl et al., 2005; Kowalczyk and Froelich, 2010; Matthey et al., 2010; Boch et al., 2011; Tremaine et al., 2011; Oster et al., 2012; and Hasegawa et al., 2014). The cave air ventilation plays a key role in controlling the variables of the cave environment in the Inazumi Cave. For instance, the outside cold air with low RH and P_{CO_2} flows into the cave when the outside temperature is colder than inside the cave, resulting in a decrease of the cave air temperature, RH and P_{CO_2} . When the temperature outside the cave is warmer than inside the cave, the air direction reverses and inflow turns into outflow, resulting in minor variation in the cave air temperature and RH. In addition, the air P_{CO_2} is increased by the supply of drip-water-origin P_{CO_2} and soil-origin P_{CO_2} percolating down to the cave through fissures and cracks. The decrease of the air temperature, RH, and P_{CO_2} at SS1 is explained by the incursion of outside air, and the increase during warm periods is due to domination by outflow regime and supply of soil-origin and drip-water-origin P_{CO_2} . The air temperature and RH at SS2 and SS3 have shown little variation compared to SS1 during the course of this research. This might be because SS2 and SS3 are farther from the cave entrance and less susceptible to the external air than SS1. Still, distinct seasonal variation in the cave air P_{CO_2} at SS2 and SS3 is the evidence of interaction of internal and external atmospheres of the cave. Varying cave air P_{CO_2} , with stable temperature and RH with increasing distance from a cave entrance, has been reported by Spötl et al. (2005) and Tremaine et al. (2011). Therefore, the Inazumi Cave has a similar air regime to these studies. Based on our monitoring, variation in cave air P_{CO_2} is regarded as the main variable for controlling the drip water geochemistry in the Inazumi Cave, and evaporation and temperature have little effect on the geochemistry.

Cave Air P_{CO_2} vs. Drip rate on Drip Water Geochemistry

The sampling method in this study is designed for determining which of cave air P_{CO_2} or drip rate has a significant effect on drip water geochemistry. If the P_{CO_2} is the main variable, the drip water geochemistry will exhibit either seasonal or diurnal variation following the variation in the cave air P_{CO_2} . If the drip rate is the main variable, the geochemistry will

always decrease in the sequential order of the handrails and glass tube to some extent, because the drip rate always decreases in its sequential order. In order to discuss these variables, we first examine the effect of the P_{CO_2} and then the drip rate.

CAVE AIR P_{CO_2}

Figure 7 provides the relation between the cave air P_{CO_2} and the drip water geochemistry at SS2 and SS3. HCO_3^- and Ca^{2+} indicate insignificant differences in the sequential order of the handrails and glass tube during high P_{CO_2} periods. As the cave air P_{CO_2} decreases, however, HCO_3^- and Ca^{2+} gradually highlight the decreasing trend and the sequential differences. This might be caused by the incursion of outside air that lowers the air P_{CO_2} and promotes CO_2 degassing and CaCO_3 precipitation from the drip-water (Spötl et al., 2005; Banner et al., 2007; Boch et al., 2011). The pronounced differences of the WBD from SS3U are measured when the cave air P_{CO_2} was < 1,500 ppm, indicating that seepage water instantaneously outgasses CO_2 once it encounters low air P_{CO_2} , implying that the WBD contains a more accurate chemical signature within the carbonate rock matrix above the cave than the dripping water. An extremely sharp decreasing trend is found at both SS2 and SS3 when the air P_{CO_2} was < 1,000 in December, implying that the very low cave air P_{CO_2} induces sudden and extreme CO_2 degassing from the drip water. These data are the first report of such an exceptional trend of the drip water geochemistry. Still, because it was measured at both dripping sites SS2 and SS3, it likely implies a general tendency for the drip water geochemistry in very low air P_{CO_2} condition at the Inazumi Cave.

Figure 8 depicts how seasonal ventilation controls cave air P_{CO_2} and the subsequent variation in drip water geochemistry. During cold periods, the incursion of outside air into the cave results in lowering cave air P_{CO_2} , HCO_3^- , and Ca^{2+} and increasing $\text{SI}_{\text{calcite}}$, hence promoting CO_2 degassing and CaCO_3 precipitation. During warm periods, outflow dominates the cave air regime, and soil-origin and drip-water-origin CO_2 flows into the cave, resulting in high air P_{CO_2} . Drip water geochemistry in such environment tends to possess high HCO_3^- , Ca^{2+} , low $\text{SI}_{\text{calcite}}$, and little CO_2 degassing and CaCO_3 precipitation are expected.

Figure 9 shows chemical evolution of HCO_3^- at SS2 and SS3 using the equation of Dulinski and Rozanski (1990). The measured and calculated values of HCO_3^- are the mean values of the drip waters in each monitoring period. Minor differences are found between the measured and calculated values during high cave air P_{CO_2} periods. This could be explained by suppression of CO_2 degassing and CaCO_3 precipitation by high air P_{CO_2} . The measured HCO_3^- gradually

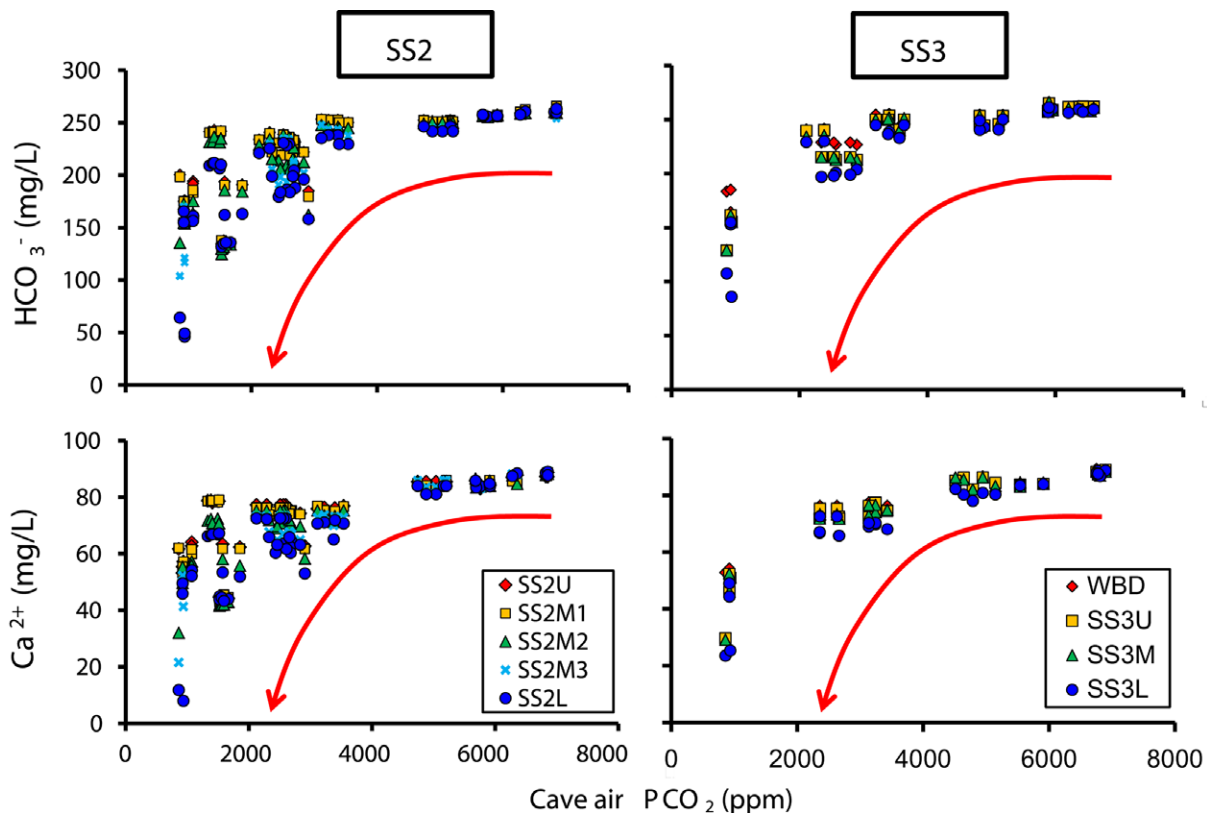


Figure 7. Relationship between the cave air P_{CO_2} , HCO_3^- , and Ca^{2+} at SS2 (left) and SS3 (right). Curved red arrows indicate the decreasing trend of HCO_3^- and Ca^{2+} following the decrease of the air P_{CO_2} .

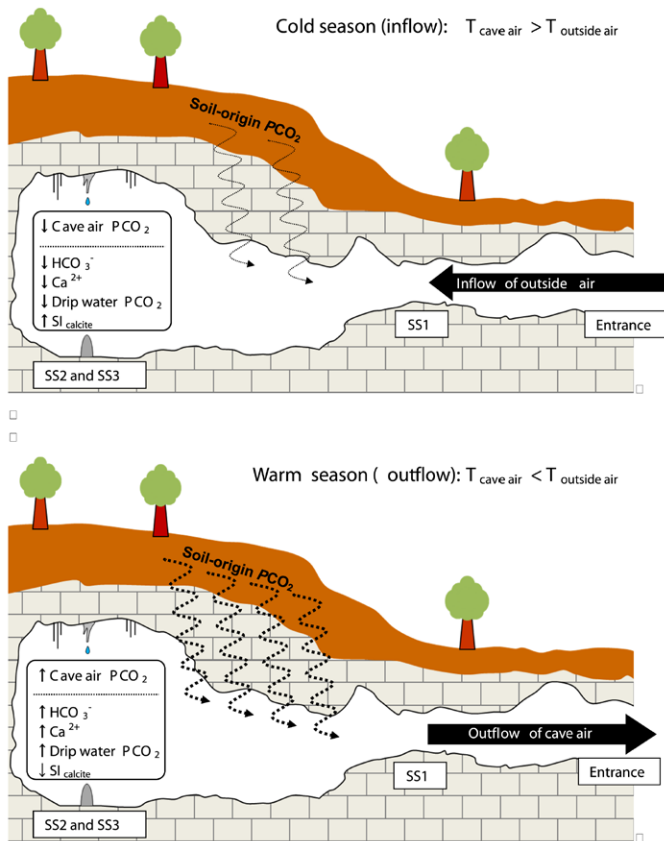


Figure 8. A conceptual diagram illustrating the relationship between seasonal cave air ventilation and drip water geochemistry at Inazumi Cave. The capital T stands for the temperature. Wavy and black dashed line represents the supply of soil air P_{CO_2} . The ventilation, driven by the temperature difference between cave and outside air, controls variation in the cave air P_{CO_2} , resulting in seasonal changes in drip water geochemistry.

decreases along with the calculated value as the air P_{CO_2} decreases. In particular, the largest differences between the measured and calculated values are found when the cave air P_{CO_2} is less than 3,000 ppm. This implies that the drip water in the natural setting with low cave air P_{CO_2} is more susceptible to forced CO_2 degassing than expected from the equation of Dulinski and Rozanski (1990). The drip water is considered to achieve chemical equilibrium with the cave atmosphere after it reaches the stalagmite (the handrails and glass tube in this research) (Milanolo and Gabrovšek, 2015). Continuous consumption of HCO_3^- in the sequential order of the handrails and glass tube and the exceptionally large difference of HCO_3^- between the measured and calculated values in December (cave air $P_{CO_2} < 1,000$ ppm) implies the possibility of forced degassing of CO_2 from the drip water during the low P_{CO_2} season.

The drip water data of P_{CO_2} at SS2 and SS3 frequently showed lower values than the air P_{CO_2} (Figs. 6A and 6B), suggesting no further CO_2 degassing out of the drip water. This tendency is contradictory to the positive values of $SI_{calcite}$ measured at SS2 and SS3 and the formation of the stalactites at SS2 and SS3 and stalagmites on the handrails at SS2. Several possible scenarios are discussed below.

(1) Prior calcite precipitation, or PCP, might have occurred within the carbonate rock matrix above the cave or on the cave ceiling. PCP has been reported as a well-known process in numerous caves and has an effect on drip water geochemistry (Fairchild et al., 2000, 2006; McDonald et al., 2007; Boch et al., 2011; Treble et al., 2015). CO_2 degassing and subsequent $CaCO_3$ precipitation are likely if the percolating water finds any passageways or air pockets with lower air P_{CO_2} within the carbonate rock matrix than the percolating water's P_{CO_2} . Such water possesses lower P_{CO_2} than the air P_{CO_2} when dripping on the stalagmite, and no further CO_2 degassing can be expected. PCP is also applicable to the formation of stalactite and flowstone, resulting in prior consumption of HCO_3^- and Ca^{2+} from the water before dripping and in decreasing the water P_{CO_2} . CO_2 is instantaneously degassed from the seepage water once the water is in contact with the cave air, and the water pH shifts toward basic from acidic (Dreybrodt and Scholz, 2011). The WBD is considered to contain the chemical signature within the carbonate rock matrix above the cave to some extent since the WBD shows higher HCO_3^- and Ca^{2+} than other dripping water at SS3 during the cold season (Fig. 5B). However,

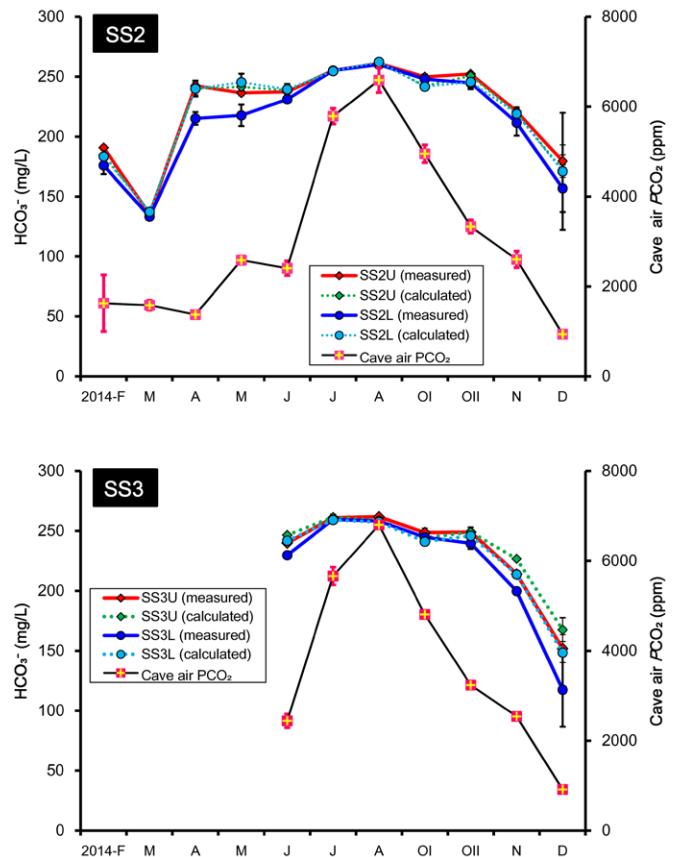


Figure 9. Comparison of the mean values of five samples of measured (solid lines) and calculated values (dashed lines) of HCO_3^- at SS2 (upper figure) and SS3 (lower figure) using the equation formulated by Dulinski and Roanski (1990) with mean values of cave air P_{CO_2} at each monitoring periods.

no pH and water temperature of the WBD are obtained due to the applied new sampling technique. An improvement of the sampling method will provide the possibility of measurement of these variables and investigation of the influence of PCP on the drip water geochemistry.

(2) The anthropogenic CO₂ temporarily increases cave air P_{CO_2} (e.g., Frisia et al., 2011). The extreme rise of the cave air P_{CO_2} in February 2014 is a typical result caused by a large number of visitors (Fig. 3A). Few tourists visited in other months during the course of this study, and the influence of human activity seems to be negligible. However, if many tourists had visited to the cave before the initiation of the monitoring, the anthropogenic CO₂ would remain in the cave for some time, contributing temporal increase of the air P_{CO_2} . The water P_{CO_2} data in such a case will be lower than the air P_{CO_2} . The Inazumi Cave is a tourist cave with large numbers of visitors in summer and autumn, and the largest gap of P_{CO_2} between drip water and cave air in August would be attributable to the visitors origin P_{CO_2} .

(3) Storage condition of sample could cause undesirable effects of CO₂ degassing from the drip water in the PET tube. If there is any small amount of air present in the PET tube or any chance where drip water contacts with external low- P_{CO_2} air, CO₂ will be stripped out of the drip water, resulting in lower P_{CO_2} than cave air P_{CO_2} when measured in the laboratory. We consider the March chemical analysis result influenced by storage artifacts. Such drip water possesses lower HCO₃⁻, Ca²⁺, and P_{CO_2} than its original state.

Sampling artifacts can be prevented by careful sample storage, however, additional air monitoring is necessary to investigate the influence of PCP and visitors on the drip water geochemistry.

Drip Rate

The drip rate decreases in the sequential order of the handrails at SS2 and the glass tube at SS3 in each monitoring period, indicating that SS2L and SS3L are permanently slow. This infers that waters at SS2L and SS3L are exposed to the cave air for longer times and that they experience thinning and widening of the water film more than other sampling sites. Such water will contain a low concentration of HCO₃⁻ and Ca²⁺ because of continuous CO₂ degassing and CaCO₃ precipitation. However, HCO₃⁻ and Ca²⁺ at SS2 and SS3 in July and August display only minor sequential variation between the handrails. HCO₃⁻ and Ca²⁺ in April and June show distinct variation in the sequential order of the handrails, even though the drip rate is similar to the one in July and August. Moreover, the drip rate at SS3 in June and July shows a rapidly decreasing trend, but HCO₃⁻ and Ca²⁺ show only minor correspondence to the drip rate. This implies that the drip rate alone has less significant influence on the variation in the drip water geochemistry than the cave air P_{CO_2} .

Table 1 presents a comparison of the correlation between the drip water geochemistry, drip rate, and cave air P_{CO_2} . The air P_{CO_2} shows higher correlations with HCO₃⁻ and Ca²⁺ than the drip rate as the overall trend. As a common feature, the correlation of both the air P_{CO_2} and drip rate increases in the sequential order at SS2 and SS3. Particularly, the correlation with the drip rate at SS2M3 and SS2L is significant. This might be caused by a decreasing trend of the drip rate from August to December corresponding with a decreasing trend of HCO₃⁻ and Ca²⁺. However, it is unusual to show partially high correlation. If the drip rate strongly affects the water geochemistry, then all sampling sections should show high correlations similar to SS2M3 and SS2L. In addition, HCO₃⁻ and Ca²⁺ at SS2 in April and June show distinct sequential variation, even though the drip rates during these periods are similar to those in July and August when HCO₃⁻ and Ca²⁺ show no minor sequential difference. Some previous studies have shown low correlation between the drip rate and drip water geochemistry, for instance, at the Obir Cave in Austria (Spötl et al., 2005) and the Crag Cave in Ireland (Baldini et al., 2006). Banner et al. (2007) conducted CaCO₃ precipitation experiment in limestone caves in Texas, USA

Table 1. Linear correlation coefficients for drip-water geochemistry, cave air P_{CO_2} vs the drip rate at SS2 and SS3. All correlation-coefficient values $p < 0.001$. Note that no data of the drip rate were obtained for the WBD due to the novel sampling method.

Drip Water Sampling Stations	HCO ₃ ⁻		Ca ²⁺	
	Cave Air P_{CO_2}	Drip Rate	Cave Air P_{CO_2}	Drip Rate
SS2U	0.66	0.33	0.73	0.37
SS2M1	0.66	0.34	0.73	0.38
SS2M2	0.77	0.53	0.79	0.56
SS2M3	0.83	0.84	0.86	0.85
SS2L	0.8	0.67	0.79	0.71
WBD	0.82	...	0.9	...
SS3U	0.84	0.64	0.87	0.7
SS3M	0.84	0.64	0.87	0.7
SS3L	0.82	0.62	0.87	0.68

and demonstrated that the CaCO_3 deposition rate correlates more with the cave air P_{CO_2} than the drip rate. Based on the previous studies above and our data from the Inazumi Cave, variation in the cave air P_{CO_2} can be regarded as the main determinant controlling drip water geochemistry.

Conclusions

Both diurnal and seasonal cave air ventilation were observed at the Inazumi Cave, and the ventilation can be attributed to the temperature difference of external and internal atmosphere of the cave, which is exclusively controlled by the opening A's air-circulation regime.

Ventilation played a key role controlling variation in cave air temperature, RH, and P_{CO_2} . While air P_{CO_2} showed remarkable diurnal and seasonal variation at all monitored sites, temperature and RH were stable at increasing distances from the cave entrances. This indicates that the cave air P_{CO_2} is the main variable that controls the variation in the drip water geochemistry at the Inazumi Cave, while temperature and evaporation have minor effects.

A novel sampling technique at SS2 and SS3 indicated seasonal variation in the cave air P_{CO_2} , not drip rate, was the main variable controlling the seasonal variation in HCO_3^- and Ca^{2+} , and that the karstic water instantaneously degassed CO_2 once in contact with low cave air P_{CO_2} .

The drip water P_{CO_2} repeatedly showed lower values than the cave air P_{CO_2} , and possible reasons are prior calcite precipitation, anthropogenic CO_2 , or storage condition of samples. Additional cave air monitoring is required to address the impact of PCP and the anthropogenic CO_2 on the drip water geochemistry.

Acknowledgements

We would like to thank Seiji Kanemitsu and the office staff working at the Inazumi Cave for permission for cave air monitoring and sampling drip water. We are also grateful to Wataru Hasegawa, an alumnus of Kyoto University, for technical advice on cave air monitoring, Shunsuke Kinoshita, a graduate student of Kyoto University, for technical support of the Raman Spectrometry, and to Horst Zwingmann, a professor the Division of Earth and Planetary Sciences of Kyoto University, and anonymous reviewers for their constructive comments related to the original version of this article. This research was financially supported by the Sasakawa Scientific Research Grant from The Japan Science Society (research number: 26-228) and Program for Next Generation World-Leading Research (NEXT Program; GR063).

References

- Baldini, J.U.L., McDermott, F., and Fairchild, I.J., 2006, Spatial variability in cave drip water hydrochemistry: Implications for stalagmite paleoclimate records: *Chemical Geology*, v. 235, p. 390–404. <http://dx.doi.org/10.1016/j.chemgeo.2006.08.005>.
- Banner, J.L., Guilfoyle, A., James, E.W., Stern, L.A., and Musgrove, M., 2007, Seasonal variations in modern speleothem calcite growth in central Texas, U.S.A.: *Journal of Sedimentary Research*, v. 77, p. 615–622. <https://doi.org/10.2110/jsr.2007.065>.
- Boch, R., Spötl, C., and Frisia, S., 2011, Origin and palaeoenvironmental significance of lamination in stalagmites from Katerloch Cave, Austria: *Sedimentology*, v. 58, p. 508–531. <https://doi.org/10.1111/j.1365-3091.2010.01173.x>.
- Burns, S.J., Fleitmann, D., Mudelsee, M., Neff, U., Matter, A., and Mangini, A., 2002, A 780-year annually resolved record of Indian Ocean monsoon precipitation from a speleothem from south Oman: *Journal of Geophysical Research: Atmospheres*, v. 107, ACL 9-1 – ACL 9-9. <https://doi.org/10.1029/2001JD001281>.
- Cai, Binggui, Pumijumngong, N., Tan, Ming, Muangsong, C., Kong, Xinggong, Jiang, Xiuyang, and Nan, Sulan, 2010, Effects of intraseasonal variation of summer monsoon rainfall on stable isotope and growth rate of a stalagmite from northwestern Thailand: *Journal of Geophysical Research: Atmospheres*, v. 115, D21104. <https://doi.org/10.1029/2009JD013378>.
- Day, C.C., and Henderson, G.M., 2011, Oxygen isotopes in calcite grown under cave-analogue conditions: *Geochimica et Cosmochimica Acta*, v. 75, p. 3956–3972. <http://dx.doi.org/10.1016/j.gca.2011.04.026>.
- Dreybrodt, W., and Scholz, D., 2011, Climatic dependence of stable carbon and oxygen isotope signals recorded in speleothems: From soil water to speleothem calcite: *Geochimica et Cosmochimica Acta*, v. 75, p. 734–752. <http://dx.doi.org/10.1016/j.gca.2010.11.002>.
- Dulinski, M., and Rozanski, K., 1990, Formation of $^{13}\text{C}/^{12}\text{C}$ isotope ratios in speleothems: a semi-dynamic model: *Radiocarbon*, v. 32, p. 7–16.
- Fairchild, I.J., Borsato, A., Tooth, A.F., Frisia, S., Hawkesworth, C.J., Huang, Yiming, McDermott, F., and Spiro, B., 2000, Controls on trace element (Sr-Mg) compositions of carbonate cave waters: implications for speleothem climate records: *Chemical Geology*, v. 166, p. 255–269. [http://dx.doi.org/10.1016/S0009-2541\(99\)00216-8](http://dx.doi.org/10.1016/S0009-2541(99)00216-8).
- Fairchild, I.J., Smith, C.L., Baker, A., Fuller, L., Spötl, C., Matthey, D., McDermott, F., and E.I.M.F. (Edinburgh Ion Microprobe Facility), 2006, Modification and preservation of environmental signals in speleothems: *Earth Science Reviews*, v. 75, p.105–153. <http://dx.doi.org/10.1016/j.earscirev.2005.08.003>.
- Frisia, S., Fairchild, I.J., Fohlmeister, J., Miorandi, R., Spötl, C., and Borsato, A., 2011, Carbon mass-balance modelling and carbon isotope exchange processes in dynamic caves: *Geochimica et Cosmochimica Acta*, v. 75, p. 380–400. <http://dx.doi.org/10.1016/j.gca.2010.10.021>.
- Fujii, A., and Nishida, T., 1999, Hydrogeology of the Inazumi, Furen and Onagara Limestone Caves, Oita Prefecture, with special reference to the history of the Inazumi Limestone Cave: Special issue of the Geological Society of Oita, Symposium on Limestone in Southwest Japan, v. 5, p. 49–68. (In Japanese)
- Hasegawa, W., Sawagaki, T., Hirakawa, K., Watanabe, Y., and Tagami, T., 2014, Description and environmental monitoring of Hokkai Cave in northern Japan: *Cave and Karst Science*, v. 41, p. 3–12.
- Hendy, C.H., 1971, The isotopic geochemistry of speleothems-I. The calculation of the effects of different mode of formation on the isotopic composition of speleothems and their applicability as paleoclimate indicators: *Geochimica et Cosmochimica Acta*, v. 35, p. 801–824. [http://dx.doi.org/10.1016/0016-7037\(71\)90127-X](http://dx.doi.org/10.1016/0016-7037(71)90127-X).
- Johnson, K.R., Hu, Chaoyong, Belshaw, N.S., and Henderson, G.M., 2006, Seasonal trace-element and stable-isotope variations in a Chinese

- speleothem: The potential for high-resolution paleomonsoon reconstruction: *Earth and Planetary Science Letters*, v. 244, p. 394–407. <http://dx.doi.org/10.1016/j.epsl.2006.01.064>.
- Kowalczyk, A.J., and Froelich, P.N., 2010, Cave air ventilation and CO₂ outgassing by radon-222 modeling: How fast do caves breathe?: *Earth and Planetary Science Letters*, v. 289, p. 209–219. <http://dx.doi.org/10.1016/j.epsl.2009.11.010>.
- Mattey, D., Lowry, D., Duffet, J., Fisher, R., Hodge, E., and Frisia, S., 2008, A 53 year seasonally resolved oxygen and carbon isotope record from a modern Gibraltar speleothem: Reconstructed drip water and relationship to local precipitation: *Earth and Planetary Science Letters*, v. 269, p. 80–95. <http://dx.doi.org/10.1016/j.epsl.2008.01.051>.
- Mattey, D.P., Fairchild, I.J., Atkinson, T.C., Latin, J.P., Ainsworth, M., and Durell, R., 2010, Seasonal microclimate control of calcite fabrics, stable isotopes and trace elements in modern speleothem from St Michaels Cave, Gibraltar, in Pedley, H.M., and Rogerson, M., eds.: *Tufas and Speleothems: Unravelling the Microbial and Physical Controls*; Geological Society London Special Publication, v. 336, p. 323–344. <https://doi.org/10.144/SP336.17>.
- McDonald, J., Drysdale, R., Hill, D., Chisari, R., and Wong, H., 2007, The hydrochemical response of cave drip waters to sub-annual and inter-annual climate variability, Wombeyan Caves, SE Australia: *Chemical Geology*, v. 244, p. 605–623. <http://dx.doi.org/10.1016/j.chemgeo.2007.07.007>.
- Mickler, P.J., Stern, L.A., and Banner, J.L., 2006, Large kinetic isotope effects in modern speleothems: *Geological Society of America Bulletin*, v. 118, p. 65–81. <https://doi.org/10.1130/B25698.1>.
- Milanolo, S., and Gabrovšek, F., 2015, Estimation of carbon dioxide flux degassing from percolating waters in a karst cave: Case study from Bijambare cave, Bosnia and Herzegovina: *Chemie der Erde*, v. 75, p. 465–474. <http://dx.doi.org/10.1016/j.chemer.2015.10.004>.
- Mishima, T., Ohsawa, S., Yamada, M., and Kitaoka, K., 2009, A new method for determination of bicarbonate ion in a small amount of environmental water samples: *Journal of Japanese Association of Hydrological Sciences*, v. 38, No.4. <https://doi.org/10.4145/jahs.38.157> (In Japanese).
- Ohsawa, S., 2009, Air circulation in limestone cave in response to speleothem growth: *Annual Report of Geological Society Oita*, v. 15, p. 1–10. (In Japanese).
- Oster, J.L., Montañez, I.P., and Kelly, N.P., 2012, Response of a modern cave system to large seasonal precipitation variability: *Geochimica et Cosmochimica Acta*, v. 91, p. 92–108. <http://dx.doi.org/10.1016/j.gca.2012.05.027>.
- Parkhurst, L., David, and Appelo, C.A.J., 2013, Description of Input and Examples for PHREEQC Version 3—A Computer Program for Speciation, Batch-Reaction, One-Dimensional Transport, and Inverse Geochemical Calculations: U.S. Geological Survey Techniques and Methods, book 6, chap. A43, p. 497. <https://pubs.usgs.gov/tm/06/a43/>.
- Proctor, C., Baker, A., and Barnes, W.L., 2002, A three thousand year record of North Atlantic climate: *Climate Dynamics*, v. 19, p. 449–454. <https://doi.org/10.1007/s00382-002-0236-x>.
- Proctor, C.J., Baker, A., Barnes, W.L., and Gilmour, M.A., 2000, A thousand year speleothem proxy record of North Atlantic climate from Scotland: *Climate Dynamics*, v. 16, p. 815–820. <https://doi.org/10.1007/s003820000077>.
- Spötl, C., Fairchild, I.J., and Tooth, A.F., 2005, Cave air control on dripwater geochemistry, Obir Cave (Austria): Implications for speleothem deposition in dynamically ventilated caves: *Geochimica et Cosmochimica Acta*, v. 69, p. 2451–2468. <http://dx.doi.org/10.1016/j.gca.2004.12.009>.
- Treble, P.C., Fairchild, I.J., Griffiths, A., Baker, A., Meredith, K.T., Wood, A., and McGuire, E., 2015, Impacts of cave air ventilation and in-cave prior calcite precipitation on Golgotha Cave dripwater chemistry, southwest Australia: *Quaternary Science Reviews*, v. 127, p. 61–72. <http://dx.doi.org/10.1016/j.quascirev.2015.06.001>.
- Treble, P., Shelley, J.M.G., and Chappell, J., 2003, Comparison of high resolution sub-annual records of trace elements in a modern (1911–1992) speleothem with instrumental climate data from southwest Australia: *Earth and Planetary Science Letters*, v. 216, p. 141–153. [http://dx.doi.org/10.1016/S0012-821X\(03\)00504-1](http://dx.doi.org/10.1016/S0012-821X(03)00504-1).
- Tremaine, D.M., Froelich, P.N., and Wang, Yang, 2011, Speleothem calcite formed in situ: Modern calibration of δ¹⁸O and δ¹³C paleoclimate proxies in a continuously-monitored natural cave system: *Geochimica et Cosmochimica Acta*, v. 75, p. 4929–4950. <http://dx.doi.org/10.1016/j.gca.2011.06.005>.
- Wang, Y.J., Cheng, H., Edwards, R.L., An, Z.S., Wu, J.Y., Shen, C.-C., and Dorale, J.A., 2001, A high-resolution absolute-dated Late Pleistocene monsoon record from Hulu Cave, China: *Science*, v. 294, p. 2345–2348. <https://doi.org/10.1126/science.1064618>.
- Wang, Xiaoxiao, Wu, Yanhung, and Shen, Licheng, 2016, Influences of air CO₂ on hydrochemistry of drip water and implications for paleoclimate study in a stream-developed cave, SW China: *Acta Geochimica*, v. 35, p. 172–183. <https://doi.org/10.1007/s11631-015-0085-z>.
- Watanabe, Y., Matsuoka, H., Sakai, S., Ueda, J., Yamada, M., Ohsawa, S., Kiguchi, M., Satomura, T., Nakai, S., Brahmantyo, B., Mayrunani, K. A., Tagami, T., Takemura, K., and Yoden, S., 2010, Comparison of stable isotope time series of stalagmite and meteorological data from West Java, Indonesia: *Paleogeography, Paleoclimatology, Paleoecology*, v. 293, p. 90–97. <http://dx.doi.org/10.1016/j.palaeo.2010.05.003>.